

**SYNTHESIS, AB INITIO STRUCTURE DETERMINATION, AND CHARACTERIZATION OF MANGANESE(III) PHENYL PHOSPHONATES****A. Cabeza¹, M.A.G. Aranda¹, S. Bruque^{1*}, D.M. Poojary^{2†}, and A. Clearfield²**¹Departamento de Química Inorgánica, Universidad de Málaga, 29071 Málaga, Spain²Department of Chemistry, Texas A & M University, College Station, Texas 77843, USA

(Refereed)

(Received September 25, 1997; Accepted October 15, 1997)

ABSTRACT

Two new manganese(III) phenyl phosphonates, $\text{Mn}(\text{HO}_3\text{PC}_6\text{H}_5)(\text{O}_3\text{PC}_6\text{H}_5)\cdot\text{H}_2\text{O}$ and $\text{Mn}(\text{HO}_3\text{PC}_6\text{H}_5)(\text{O}_3\text{PC}_6\text{H}_5)$, were synthesized. The crystal structure of $\text{Mn}(\text{HO}_3\text{PC}_6\text{H}_5)(\text{O}_3\text{PC}_6\text{H}_5)$ was solved ab initio from powder X-ray diffraction data. This compound crystallizes in the triclinic system, $a = 10.2149(5)$, $b = 15.0028(8)$, $c = 5.0324(3)$ Å, $\alpha = 95.563(4)^\circ$, $\beta = 116.858(4)^\circ$, $\gamma = 95.684(5)^\circ$, $V = 675.87(6)$ Å³, space group $P\bar{1}$, and $Z = 2$. The final agreement factors were $R_{\text{WP}} = 12.8\%$, $R_{\text{P}} = 9.1\%$, and $R_{\text{F}} = 3.2\%$. There are 22 non-hydrogen atoms in the asymmetric part of the unit cell, and the positional parameters were refined with the help of soft constraints. The octahedral manganese coordination spheres are distorted due to the Jahn-Teller effect. The structure of this organic-inorganic compound is layered. The thermal behavior of $\text{Mn}(\text{HO}_3\text{PC}_6\text{H}_5)(\text{O}_3\text{PC}_6\text{H}_5)\cdot\text{H}_2\text{O}$ was studied and its thermal decomposition product was identified. © 1998 Elsevier

*Science Ltd***KEYWORDS:** A. layered compounds, B. chemical synthesis, C. X-ray diffraction**INTRODUCTION**

Metal organo-phosphonates have the general formula $\text{M}_x(\text{H}_y\text{O}_3\text{PR})_z\cdot\text{H}_2\text{O}$, where R is an organic group covalently bonded to the phosphorus atom. The different M/P ratios, the

*To whom correspondence should be addressed.

†Current address: Symyx Technologies, 3100 Central Expressway, Santa Clara, CA 95051, USA.

presence or absence of hydrogen atoms on the phosphonate groups, and the variable water content give rise to many stoichiometries and diverse structural types. These materials are being actively studied due to their potential uses for various chemical processes [1,2]. Although several types of structures are known, most metal phosphonates have layered structures. These layered materials can act as hosts in intercalation reactions and thus may serve as sorbents, catalysts, and ion exchangers [3–10].

Tetravalent metal phosphonates have been widely characterized [11–13] and their structures are closely related to that of the parent zirconium hydrogen phosphate hydrate [14]. More recently, several divalent metal phosphonates have been studied [15–18]. There also are reports on materials based on trivalent metals Fe [19], Ln [9,20], Al [21–27], and Bi [28], but, as far as we are aware, there are no reported studies on Mn(III) phosphonates. In this paper, we report the synthesis and characterization of a new Mn(III) phenyl phosphonate, $\text{Mn}(\text{HO}_3\text{PC}_6\text{H}_5)(\text{O}_3\text{PC}_6\text{H}_5)\cdot\text{H}_2\text{O}$, and its dehydrated derivative, $\text{Mn}(\text{HO}_3\text{PC}_6\text{H}_5)(\text{O}_3\text{PC}_6\text{H}_5)$.

EXPERIMENTAL

Synthesis. Chemicals of reagent quality were obtained from commercial sources and used without purification. Hydrated manganese(III) phenyl phosphonate was synthesized by adding 75 mL of a solution of phenyl phosphonic acid (1 M) to 1 g of orange-brown manganese(III) acetate dihydrate (3.73 mmol). The resulting Mn:P molar ratio was 1:20. In these conditions, a poorly crystalline pink-violet precipitate was obtained. The mixture was refluxed for several days and the crystallinity of the solid was routinely checked by powder diffraction. By increasing the refluxing time, the diffraction peaks of the precipitate become slightly sharper. However, after 10 days, a small amount of manganese(II) phenyl phosphonate was detected in the pattern. This reduction of Mn(III) to Mn(II) was avoided by adding 1 mL of concentrated nitric acid to the refluxing mixture every 2 days. The overall refluxing time was 20 days. The solid was filtered, washed with water (three times) and acetone (two times), and air dried. Pink-brown anhydrous manganese(III) phenyl phosphonate was obtained by heating the hydrate at 170°C for 4 h.

Chemical Analysis. The sample was dissolved in HNO_3 (1:1) and the manganese content was determined by atomic absorption spectroscopy. Carbon and hydrogen contents were determined by elemental chemical analysis with a Perkin-Elmer 240 analyzer. The phosphorus content was deduced from the carbon percentage found, assuming a C:P molar ratio of 6:1. The water content was determined from the weight loss in the TGA curve and from static heating. Analytical data: Mn, 13.60%; P, 15.85%; C, 36.92%; H, 3.40%. Calcd. for $\text{Mn}(\text{HO}_3\text{PC}_6\text{H}_5)(\text{O}_3\text{PC}_6\text{H}_5)\cdot\text{H}_2\text{O}$: Mn, 14.24%; P, 16.06%; C, 37.30%; H, 3.37%; H_2O , 4.67%.

Physical Characterization. TGA and DTA data were collected with a Rigaku Thermoflex apparatus at the heating rate of 10 Kmin^{-1} in air with calcined Al_2O_3 as the internal reference standard. Infrared (IR) spectra were recorded on a Perkin-Elmer 883 spectrometer in the spectral range $4000\text{--}400 \text{ cm}^{-1}$, using dry KBr pellets containing 2% of the sample. The X-ray diffraction (XRD) data for $\text{Mn}(\text{HO}_3\text{PC}_6\text{H}_5)(\text{O}_3\text{PC}_6\text{H}_5)\cdot\text{H}_2\text{O}$ and $\text{Mn}(\text{HO}_3\text{PC}_6\text{H}_5)(\text{O}_3\text{PC}_6\text{H}_5)$ were collected on a Rigaku Ru-200 automated powder diffractometer. The source was a rotating anode generator operated at 50 kV and 180 mA, with a

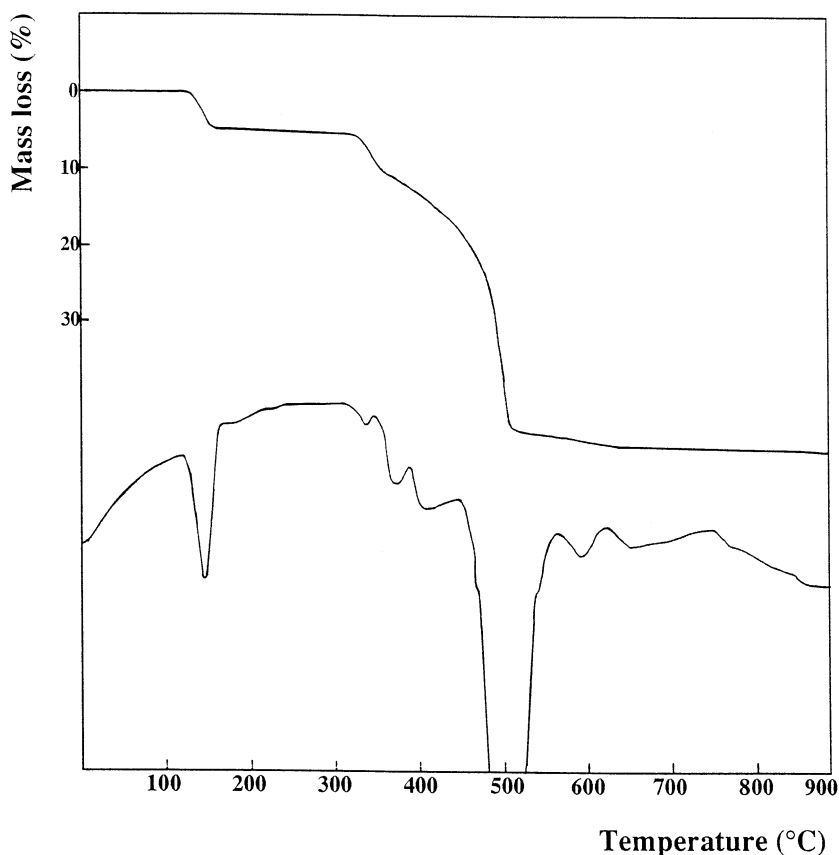


FIG. 1
TGA-DTA curves for $\text{Mn}(\text{HO}_3\text{PC}_6\text{H}_5)(\text{O}_3\text{PC}_6\text{H}_5)\cdot\text{H}_2\text{O}$.

copper target and graphite monochromator. XRD data were recorded between 4° and 80° (2θ), with a 0.01° step size and 10-s counting time.

RESULTS AND DISCUSSION

Thermal Study. DTA-TGA curves for $\text{Mn}(\text{HO}_3\text{PC}_6\text{H}_5)(\text{O}_3\text{PC}_6\text{H}_5)\cdot\text{H}_2\text{O}$ are shown in Figure 1. There are three main mass losses in the TGA curve that are associated with several endotherms. The first endotherm centered at 140°C is due to the release of the water molecule, giving crystalline $\text{Mn}(\text{HO}_3\text{PC}_6\text{H}_5)(\text{O}_3\text{PC}_6\text{H}_5)$. The observed mass loss is 5.0% in agreement with a calculated value of 4.67%. There are three processes taking place between 300 and 600°C : first, the release of a water molecule formed by the condensation of two hydrogen phosphonate groups; second, the pyrolysis of the organic groups; and third the reduction of Mn(III) to Mn(II). The second endotherm centered at 340°C probably corresponds to the condensation process, and the strong endotherm at 515°C is due to the pyrolysis. However, these three processes overlap, so it is not possible to distinguish which of the endotherms corresponds to the reduction of Mn(III). The X-ray profile for the sample heated at 800°C is completely explained by the $\text{Mn}(\text{PO}_3)_2$ powder pattern (PDF data base

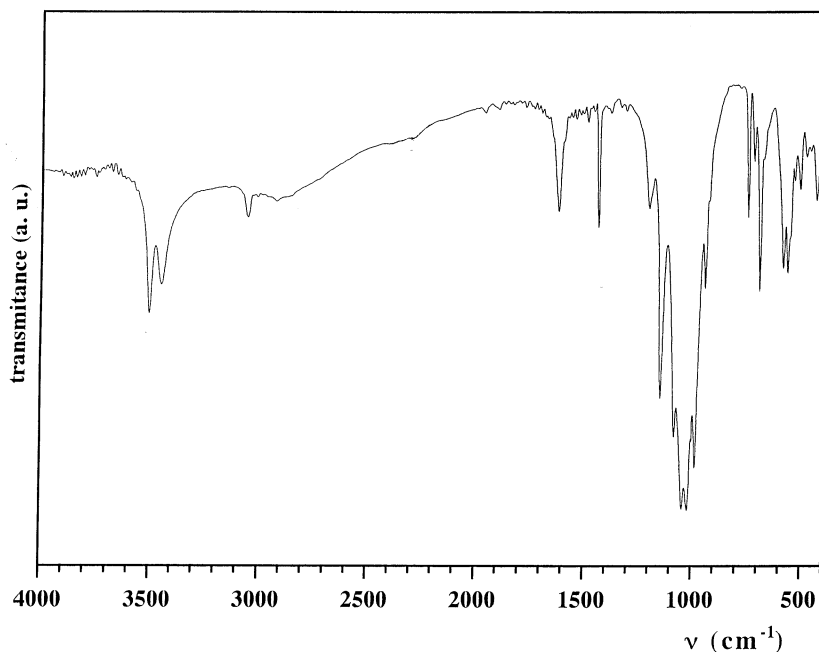
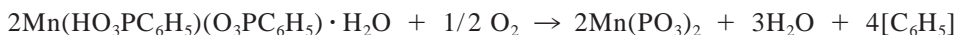


FIG. 2
IR spectrum for $\text{Mn}(\text{HO}_3\text{PC}_6\text{H}_5)(\text{O}_3\text{PC}_6\text{H}_5)\cdot\text{H}_2\text{O}$.

29–0892). The total mass loss at 800°C is 46.0%, which is close to the theoretical value of 44.8% calculated for the overall thermal decomposition of $\text{Mn}(\text{HO}_3\text{PC}_6\text{H}_5)(\text{O}_3\text{PC}_6\text{H}_5)\cdot\text{H}_2\text{O}$, to give $\text{Mn}(\text{PO}_3)_2$:



IR Study. The IR spectrum of $\text{Mn}(\text{HO}_3\text{PC}_6\text{H}_5)(\text{O}_3\text{PC}_6\text{H}_5)\cdot\text{H}_2\text{O}$ is shown in Figure 2. Two sharp bands at 3510 and 3460 cm^{-1} are observed in the H–O stretching vibration region; they are due to the asymmetric and symmetric O–H stretching vibration of the hydration water. The position at high frequencies and small width of these bands are consistent with zeolitic water in the structure that is interacting very weakly by hydrogen bonds. The sharp band at 3066 cm^{-1} is characteristic of the C–H stretching vibrations of the phenyl ring. Two broad bands at 2900 and 2300 cm^{-1} are usually related to the hydrogen phosphonate groups, HO_3PC . The H–O–H bending band is evident at 1620 cm^{-1} . The bands at 1487 and 1437 cm^{-1} are due to the C–C skeletal vibrations of the phenyl rings, and the set of bands in the 1200 – 900 cm^{-1} region are due to the different P–O stretching vibrations of the phosphonate groups.

Structure Determination of $\text{Mn}(\text{HO}_3\text{PC}_6\text{H}_5)(\text{O}_3\text{PC}_6\text{H}_5)$. Powder diffraction data were mathematically stripped off the $\text{K}\alpha_2$ contribution, and peak picking was conducted by a modification of the double-derivative method [29]. The powder pattern was indexed by the Ito method [30] on the basis of the first 20 observed lines. Both compounds were indexed in a triclinic unit cell, space group $\overline{P1}$, with lattice parameters $a = 5.081$, $b = 15.246$, $c = 4.891$

TABLE 1
 Positional Parameters for $\text{Mn}(\text{HO}_3\text{PC}_6\text{H}_5)(\text{O}_3\text{PC}_6\text{H}_5)$
 in Space Group $P\bar{1}$, with $a = 10.2149(5)$,
 $b = 15.0028(8)$, $c = 5.0324(3)$ Å,
 $\alpha = 95.563(4)^\circ$, $\beta = 116.858(4)^\circ$,
 $\gamma = 95.684(4)^\circ$, $V = 675.87(6)$ Å³

Atom	<i>x</i>	<i>y</i>	<i>z</i>
Mn(1)	0.00	0.00	0.00
Mn(2)	0.50	0.00	0.00
P(1A)	-0.0988(8)	0.1044(5)	0.431(2)
O(1A)	-0.055(2)	0.1003(10)	0.165(3)
O(2A)	-0.252(1)	0.0456(9)	0.333(3)
O(3A)	0.021(1)	0.0736(8)	0.708(3)
C(1A)	-0.101(1)	0.2234(5)	0.517(4)
C(2A)	0.027(1)	0.2853(8)	0.588(5)
C(3A)	0.028(1)	0.3783(7)	0.658(4)
C(4A)	-0.089(2)	0.4038(7)	0.711(4)
C(5A)	-0.227(1)	0.3480(9)	0.554(5)
C(6A)	-0.236(1)	0.2586(7)	0.428(4)
P(1B)	0.3968(8)	0.1091(5)	0.433(2)
O(1B)	0.443(1)	0.0911(9)	0.193(3)
O(2B)	0.241(1)	0.0518(9)	0.334(3)
O(3B)	0.505(1)	0.0802(8)	0.742(3)
C(1B)	0.389(2)	0.2269(6)	0.510(3)
C(2B)	0.462(2)	0.2737(8)	0.809(2)
C(3B)	0.487(2)	0.368(8)	0.855(3)
C(4B)	0.402(2)	0.4140(6)	0.619(4)
C(5B)	0.301(2)	0.3644(9)	0.340(3)
C(6B)	0.311(2)	0.2728(8)	0.275(2)

Note: U_{iso} for Mn = 0.015(2) Å², U_{iso} for other atoms = 0.003(1) Å².

Å, $\alpha = 97.36^\circ$, $\beta = 107.832^\circ$, $\gamma = 90.26^\circ$, $V = 357.0$ Å³, $Z = 1$, and V_{at} (volume per non-hydrogen atom) = 16.2 Å³, $M(20) = 52$, for $\text{Mn}(\text{HO}_3\text{PC}_6\text{H}_5)(\text{O}_3\text{PC}_6\text{H}_5)\cdot\text{H}_2\text{O}$ and $a = 5.112$, $b = 4.966$, $c = 5.043$ Å, $\alpha = 94.96^\circ$, $\beta = 116.92^\circ$, $\gamma = 95.21^\circ$, $V = 339.1$ Å³, $Z = 1$, $V_{\text{at}} = 16.1$ Å³, $M(20) = 30$ for $\text{Mn}(\text{HO}_3\text{PC}_6\text{H}_5)(\text{O}_3\text{PC}_6\text{H}_5)$. It has to be emphasized that these unit cells require $Z = 1$ and that these unit-cell parameters did not index several low intensity peaks along the a axis; therefore, these are subcells of the true larger unit cells.

The structure of $\text{Mn}(\text{HO}_3\text{PC}_6\text{H}_5)(\text{O}_3\text{PC}_6\text{H}_5)$ was solved using the initial unit cell ($a = 5.112$, $b = 4.966$, $c = 5.043$ Å, $\alpha = 94.96^\circ$, $\beta = 116.92^\circ$, $\gamma = 95.21^\circ$). In this simplified cell (the lattice has $Z = 1$), manganese and the hydrogen of the phosphonate groups should be located at an inversion center. Integrated intensities were extracted from a limited range, $4^\circ < 2\theta < 50^\circ$, by the decomposition (MLE) method as described in ref. 31. This procedure gave 10 single indexed nonoverlapped reflections. The intensities of these reflections were used as a minimal data set for structure analysis in the TEXSAN [32] series of single crystal programs. However, in $P\bar{1}$ with $Z = 1$, the Mn must lie on a center of symmetry or (0, 0, 0). A Patterson map with Mn at (0, 0, 0) yields the position of a P atom at 3.3 Å from Mn. The

TABLE 2
Some Bond Distances (Å) and Angles (°) for Mn(HO₃PC₆H₅)(O₃PC₆H₅)

Mn1–O(1A) × 2	1.900(12)	O(1A)–Mn1–O(1A)	180.0	O(3A)–Mn1–O(3A)	180.0
Mn1–O(3A) × 2	1.993(11)	O(1A)–Mn1–O(3A) × 2	89.7(4)	O(3A)–Mn1–O(2B) × 2	89.6(5)
Mn1–O(2B) × 2	2.259(10)	O(1A)–Mn1–O(3A) × 2	90.3(4)	O(3A)–Mn1–O(2B) × 2	90.4(5)
		O(1A)–Mn1–O(2B) × 2	89.2(5)	O(2B)–Mn1–O(2B)	180.0
		O(1A)–Mn1–O(2B) × 2	90.3(4)		
Mn2–O(2A) × 2	2.299(10)	O(2A)–Mn2–O(2A)	180.0	O(1B)–Mn2–O(1B)	180.0
Mn2–O(1B) × 2	1.887(12)	O(2A)–Mn2–O(1B) × 2	92.4(5)	O(1B)–Mn2–O(3B) × 2	88.2(4)
Mn2–O(3B) × 2	1.869(11)	O(2A)–Mn2–O(1B) × 2	87.6(5)	O(1B)–Mn2–O(3B) × 2	91.8(4)
		O(2A)–Mn2–O(3B) × 2	92.4(5)	O(3B)–Mn2–O(3B)	180.0
		O(2A)–Mn2–O(3B) × 2	87.6(5)		
P(1A)–O(1A)	1.590(9)	O(1A)–P(1A)–O(2A)	111.7(7)	O(1A)–P(1A)–C(1A)	103.2(6)
P(1A)–O(2A)	1.553(8)	O(1A)–P(1A)–O(3A)	110.5(7)	O(2A)–P(1A)–C(1A)	112.1(6)
P(1A)–O(3A)	1.535(9)	O(2A)–P(1A)–O(3A)	109.3(7)	O(3A)–P(1A)–C(1A)	109.3(7)
P(1A)–C(1A)	1.801(7)				
P(1B)–O(1B)	1.541(9)	O(1B)–P(1B)–O(2B)	108.0(7)	O(1B)–P(1B)–C(1B)	109.3(7)
P(1B)–O(2B)	1.559(9)	O(1B)–P(1B)–O(3B)	112.4(8)	O(2B)–P(1B)–C(1B)	110.4(7)
P(1B)–O(3B)	1.546(9)	O(2B)–P(1B)–O(3B)	107.7(7)	O(3B)–P(1B)–C(1B)	109.4(6)
P(1B)–C(1B)	1.782(7)				

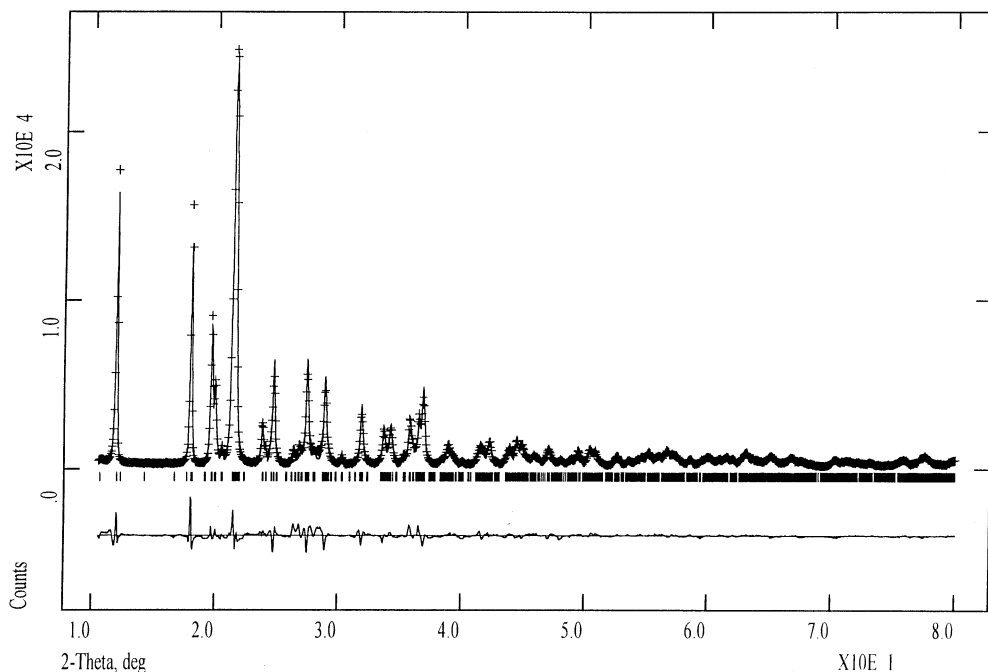


FIG. 3

Observed, calculated, and difference powder XRD profiles for Mn(HO₃PC₆H₅)(O₃PC₆H₅). The tick marks are calculated 2θ angles for Bragg peaks.

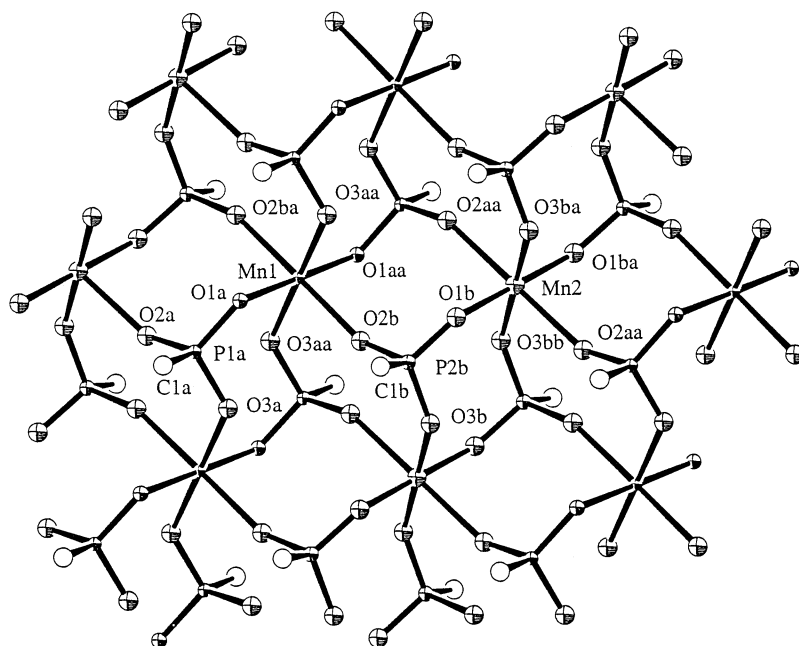


FIG. 4

Atoms arrangement within a layer of $\text{Mn}(\text{HO}_3\text{PC}_6\text{H}_5)(\text{O}_3\text{PC}_6\text{H}_5)$ (*ac* plane).

remaining atoms in the phenyl phosphonate group were positioned by modeling and input into GSAS [33] for Rietveld refinement. The refinement was performed using the following soft constraints in bonding distances [P–O, 1.53(1) Å; P–C, 1.80(1) Å; C–C, 1.40(1) Å] and nonbonding distances [Mn···P, 3.30(3) Å; O···O, 2.55(1) Å; C···C, 2.40(1) Å; and C···C, 2.78(1) Å]. Initially, the weight for the soft constraints was high, 2000, but, as the refinement progressed, it was reduced to a final value of 500. Refinement of overall parameters (scale factor, unit cell, background, zero-point error, preferred orientation along [010], and peak shape parameters) converged. In refining the atomic positions, R_{WP} [34] fell to 20%. At this stage, we introduced the refined atomic positions as the initial model into a new doubled unit cell that indexed all the peaks. With this new cell (doubled *a* axis and $Z = 2$), the final refinement converged to $R_{\text{WP}} = 12.8\%$, $R_{\text{P}} = 9.1\%$, and $R_{\text{F}} = 3.2\%$. One isotropic thermal parameter was refined for manganese atoms and another for the rest of atoms. Final positional and thermal parameters are presented in Table 1. The bond lengths and angles are given in Table 2. The Rietveld refinement plot is shown in Figure 3.

Crystal Structure of $\text{Mn}(\text{HO}_3\text{PC}_6\text{H}_5)(\text{O}_3\text{PC}_6\text{H}_5)$. This compound has 22 atoms in the asymmetric part of the unit cell. There are two crystallographic independent manganese atoms occupying the special positions at (0 0 0) and (1/2 0 0) and two independent phosphonate groups, one being protonated. $\text{Mn}(\text{HO}_3\text{PC}_6\text{H}_5)(\text{O}_3\text{PC}_6\text{H}_5)$ has a layered structure; a view of a portion of a layer is shown in Figure 4. The layer arrangement along the *b* axis is displayed in Figure 5. This layered structure is very similar to those of $\alpha\text{-Zr}(\text{O}_3\text{POH})_2 \cdot \text{H}_2\text{O}$ [14] and $\text{M}(\text{O}_3\text{PC}_6\text{H}_5)_2$ ($\text{M} = \text{Zr}, \text{U}$) [13,35]. Three manganese atoms form a pseudo-equilateral triangle with a phosphonate group approximately in the center.

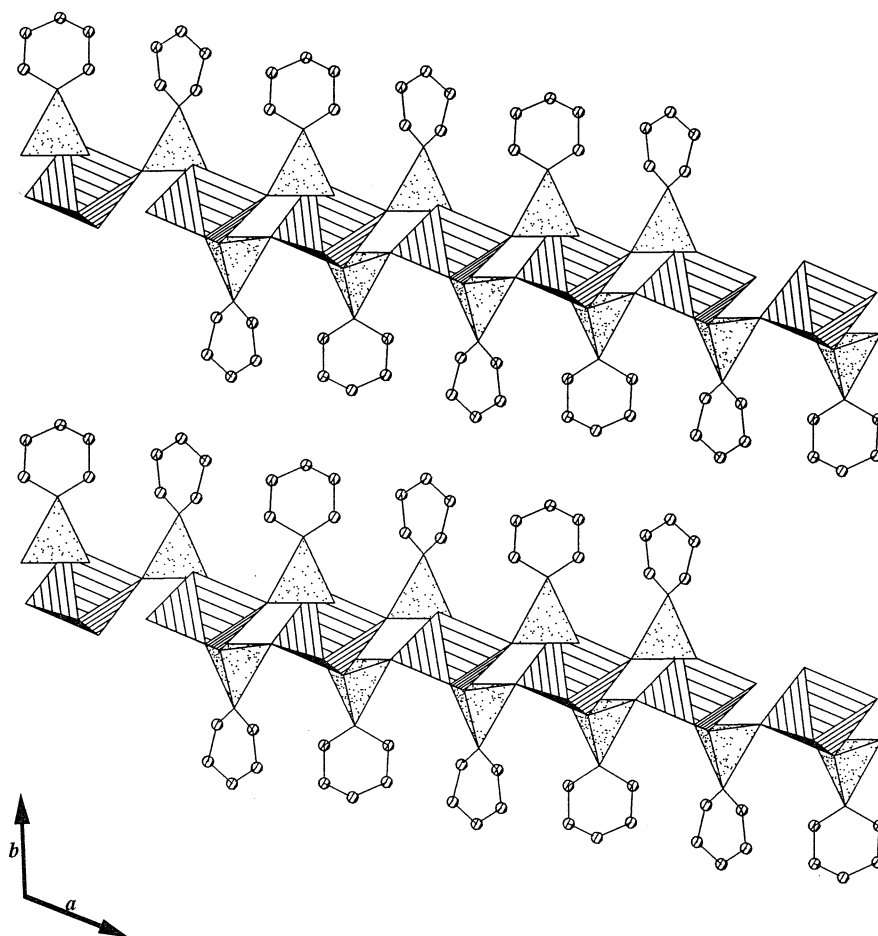


FIG. 5
 $\langle 001 \rangle$ polyhedral view (b axis vertical) of $\text{Mn}(\text{HO}_3\text{PC}_6\text{H}_5)(\text{O}_3\text{PC}_6\text{H}_5)$.

Around a given Mn atom, there are six such triangles, in which the P atoms are located approximately at 1.6 \AA , alternately above and below of the ac plane. The three oxygen atoms of the phosphonate groups are bonded to the Mn atoms, resulting in a distorted octahedral environment for both Mn(1) and Mn(2). Mn^{3+} is a d^4 cation and, hence, it displays a Jahn-Teller distortion. The Mn(1)–O bond distances are 2×1.88 , 2×2.04 , and $2 \times 2.22 \text{ \AA}$, showing an orthorhombic $[2 + 2 + 2]$ distortion mode for Mn(1). The Mn(2)–O bond distances are 4×1.88 and $2 \times 2.30 \text{ \AA}$ Mn(2), indicating that the Mn(2) environment is better described by a tetragonal $[4 + 2]$ distortion mode. From the examination of the P–O and Mn–O bond distances, it is unclear which oxygen bonds to the proton to give the hydrogen phosphonate groups. It is very likely that H is bonded to O(2B) or O(2A), as they are weakly bonded to the manganese atoms through the long Jahn-Teller distorted bond. However, it is not possible to distinguish between these two possibilities. In fact, acid protons may be randomly distributed between two oxygens, as in $\text{La}(\text{HO}_3\text{PC}_6\text{H}_5)(\text{O}_3\text{PC}_6\text{H}_5)$ [9]. As can be

seen in Figure 5, the phenyl groups are oriented away from the *ac* plane toward to the interlamellar space and are separated by approximately 5 Å along the *a*-axis direction.

The XRD pattern of $\text{Mn}(\text{HO}_3\text{PC}_6\text{H}_5)(\text{O}_3\text{PC}_6\text{H}_5)\cdot\text{H}_2\text{O}$ has been indexed in a subcell, and it is necessary to double it to account for all peaks of the patterns. The attempts to solve the structure ab initio from powder diffraction data have been unsuccessful. However, the similarities between the powder profiles of the hydrated and anhydrous materials and between the unit-cell dimensions strongly suggest very similar layered structures, with minor changes upon water release.

ACKNOWLEDGMENT

We thank NATO for funding through the NATO CRG program 951242. The work in Málaga also was supported by the research Grants FQM-113 of Junta de Andalucía and PB93/1245 of CICYT from MEC. D.M.P. and A.C. thank the R.A. Welch Foundation for support of this study under Grant A673.

REFERENCES

1. M. Thompson, *Chem. Mater.* **6**, 1168 (1994).
2. A. Clearfield, *Comments Inorg. Chem.* **10**, 89 (1990); *Curr. Opin. Solid State Mater. Sci.* **1**, 268–278 (1996).
3. A. Clearfield, *Inorganic Ion Exchange Materials*, CRC Press, Boca Rata, FL (1982).
4. (a) A. Clearfield, in *Design of New Materials*, ed. D.L. Locke and A. Clearfield, Plenum, New York (1986). (b) L. Kullberg and A. Clearfield, *Solv. Extr. Ion Exch.* **7**, 527 (1987).
5. G.L. Rosenthal and J. Caruso, *Inorg. Chem.* **31**, 144 (1992).
6. Y. Zhang and A. Clearfield, *Inorg. Chem.* **31**, 2821 (1992).
7. D.A. Burwell, K.G. Valentine, J.H. Timmermans, and M.E. Thompson, *J. Am. Chem. Soc.* **114**, 4144 (1992).
8. G. Cao and T.E. Mallouk, *Inorg. Chem.* **30**, 1434 (1991).
9. R. Wang, Y. Zhang, H. Hu, R.R. Frausto, and A. Clearfield, *Chem. Mater.* **4**, 864 (1992).
10. K.J. Langlely, P.J. Squattrito, F. Adani, and E. Montoneri, *Inorg. Chim. Acta* **253**, 77 (1996).
11. M.B. Dines and P.D. Giacomo, *Inorg. Chem.* **20**, 92 (1981).
12. D.A. Burwell and M.E. Thompson, *Chem. Mater.* **3**, 14 (1991) and references therein.
13. A. Cabeza, M.A.G. Aranda, F.M. Cantero, D. Lozano, M. Martínez-Lara, and S. Bruque, *J. Solid State Chem.* **121**, 181 (1996).
14. (a) A. Clearfield and G.D. Smith, *Inorg. Chem.* **8**, 431 (1969). (b) A. Clearfield and J. M. Troup, *Inorg. Chem.* **16**, 3311 (1977); (c) G. Cao, H.-G. Hong, and T.E. Mallouk, *Accounts Chem. Res.* **25**, 420 (1992).
15. (a) G. Cao, H. Lee, V.M. Lynch, and T.E. Mallouk, *Inorg. Chem.* **27**, 2781 (1988). (b) G. Cao, V.M. Lynch, and C.N. Yacullo, *Chem. Mater.* **5**, 1000 (1993); (c) D.M. Poojary and A. Clearfield, *J. Am. Chem. Soc.* **117**, 11278 (1995).
16. L.J. Bideau, C. Payen, B. Bujoli, P. Palvadeau, and J. Rouxel, *J. Magn. Magn. Mater.* **140–144**, 1719 (1995).
17. L.J. Bideau, C. Payen, P. Palvadeau, and B. Bujoli, *Inorg. Chem.* **33**, 4885 (1994).
18. S. Drumel, P. Janvier, D. Deniaud, and B. Bujoli, *J. Chem. Soc., Chem. Commun.* 1051 (1995).
19. B. Bujoli, P. Palvadeau, and J. Rouxel, *Chem. Mater.* **2** (5), 582 (1990).
20. G. Cao, H. Lee, V.M. Lynch, J.S. Swinnea, and T.E. Mallouk, *Inorg. Chem.* **29**, 2112 (1990).
21. J.E. Haky, J.B. Brady, N. Dando, and D. Weaver, *Mater. Res. Bull.* **32**, 297 (1997).
22. L. Raki and C. Detellier, *Chem. Comm.* **21**, 2475 (1996).

23. A. Cabeza, M.A.G. Aranda, S. Bruque, D.M. Poojary, A. Clearfield, and J. Sanz, submitted to *Inorg. Chem.*
24. K. Maeda, Y. Kiyozumi and F. Mizukami, *Angew. Chem., Int. Ed. Engl.* **33**, 2335 (1994).
25. K. Maeda, J. Akimoto, Y. Kiyozumi, and F. Mizukami, *Angew. Chem., Int. Ed. Engl.* **34**, 1199 (1995).
26. L.-J. Sawers, V.J. Carter, A.R. Armstrong, P.G. Bruce, P.A. Wright, and B.E. Gore, *J. Chem. Soc., Dalton Trans.* 3159 (1996).
27. K. Maeda, J. Akimoto, Y. Kiyozumi, and F. Mizukami, *J. Chem. Soc., Chem. Commun.*, 1033 (1995).
28. P. Janvier, S. Drumel, Y. Piffard, and B. Bujoly, *C. R. Acad. Sci. (Paris)* **320** Serie II, 29 (1995).
29. C.L. Mellory and R.L. Synder, *Adv. X-ray Anal.* **23**, 121 (1979).
30. J.W. Visser, *J. Appl. Crystallogr.* **2**, 89 (1969).
31. P.R. Rudolf and A. Clearfield, *Inorg. Chem.* **28**, 1706 (1989).
32. Crystal Structure Analysis Package, Molecular Structure Corporation, 1985 and 1992.
33. A.C. Larson and R. B. Von Dreele, Report LA-UR-86-748, Los Alamos National Laboratory, 1987.
34. (a) H.M. Rietveld, *J. Appl. Crystallogr.* **2**, 65 (1969). (b) *The Rietveld Method*, ed. R.A. Young, Oxford University Press, Oxford (1993).
35. D.M. Poojary, H.-L. Hu, F.L. Campbell, III, and A. Clearfield, *Acta Crystallogr. B* **49**, 996 (1993).